Localizing the NADP+ binding site on the MurB enzyme by NMR

NMR resonances of backbone nuclei have been assigned for >95% of the residues in oxidized, substrate-free, perdeuterated $^{13}C/^{15}N$-labelled MurB (347 residues). A novel approach utilizing minimum chemical shift changes was employed to localize the NADP+ binding site on MurB.

Sir—UDP-*N*-acetylenolpyruvylglucosamine reductase (MurB), a monomeric flavoprotein, is involved in the synthesis of the peptidoglycan layer of the bacterial cell wall through the reduction of UDP-*N*-acetylenolpyruvylglucosamine (UNAGEP) to UDP-*N*-acetyl muramic acid (UNAM)[1]. Thus, MurB represents a potentially novel anti-infective drug target. Crystal structures have recently been determined for both substrate-free MurB[2] and UNAGEP-complexed MurB[3] to resolutions of, respectively, 3.0 Å and 2.7 Å. NADPH is also a substrate for MurB; to date, no crystal structure has been determined for NADP+-complexed MurB. Therefore, we have initiated NMR studies on MurB both to identify and to characterize the NADP+ binding site on this important enzyme.

Structural analysis by NMR is challenging for large proteins because of both increased spectral overlap and decreased sensitivity. In general, spectral overlap has been mitigated by two developments: the convenient expression of proteins uniformly enriched in ^{13}C and ^{15}N isotopes[4,5]; and the introduction of both multi-dimensional, multi-resonance scalar correlation[6,7] and NOE experiments[8,9]. For these experiments, sensitivity is significantly affected by T_2 relaxation of the backbone nuclei. Increases in both sensitivity[10–12] and resolution[13] have been obtained for backbone resonances in large proteins by deuteration. Utilizing both perdeuteration and $^{13}C/^{15}N$ isotopic labelling, sequential backbone resonances have been assigned for oxidized, substrate-free MurB from *Escherichia coli*[14].

Resonance assignment of MurB

Sequential backbone resonance assignments have been determined for >95% of the residues in *E. coli* MurB[14]. An analysis of ^{15}N relaxation data[15] indicates that, at 30.0 °C, MurB has an effective isotropic rotational correlation time of 18–19 ns. With MurB, establishing sequential backbone resonance assignments, although greatly aided by perdeuteration in terms of sensitivity, was complicated by several factors: (i) the sheer number of residues that comprise the monomeric MurB protein; (ii) conformational heterogeneity in certain regions; and (iii) a decrease in the number of resonance types through which amino-acid spin systems can be sequentially linked. The latter factor results from the elimination by perdeuteration of all $H_{\alpha/\beta}$ resonances.

In summary, resonances have been assigned for one or more backbone atoms in 334 out of the 347 MurB residues (96%). The number of residues for which a specific atom has been assigned is as follows: 309 for H_N and N (94%); 315 for CO (91%); 331 for C_α (95%); and 297 for C_β (93%). C_γ resonances have been assigned for 89 residues to aid the sequential assignment process (a detailed listing of the resonance assignments for substrate-free, perdeuterated MurB will be published elsewhere).

NADP+ binding characteristics

Multiple-point titration experiments with NADP+ have been conducted on MurB. Fig. 1 demonstrates that NADP+ is in slow exchange between free and MurB-complexed forms. The K_d for NADP+ binding to the oxidized form of MurB is ~2 μM at pH 7.5 (J. Robertson, data not shown). If the on-rate of NADP+ were diffusion controlled, a K_d this large would suggest intermediate to fast exchange. The counter-observation of slow exchange, however, suggests that NADP+ may bind to MurB utilizing a gated or 'latch' mechanism, analogous to that proposed for UNAGEP[2].

NADP+ binding site

No crystal structure has been reported to date for NADP+-complexed

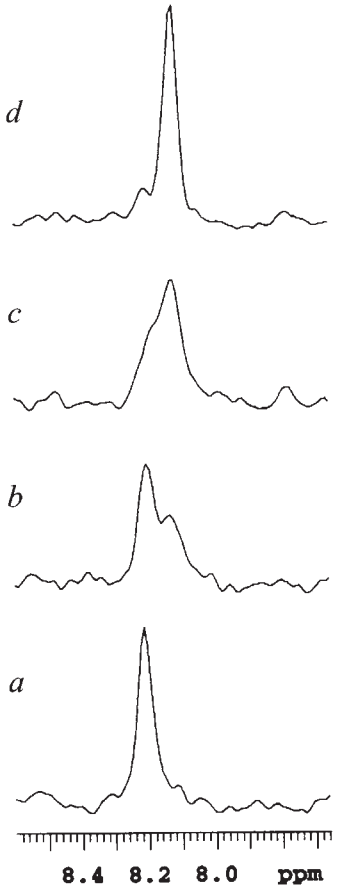

Fig. 1 F_2 traces from 2D ^1H-^{15}N HSQC spectra show the Glu 316 amide-proton resonance at the following NADP+:MurB molar ratios: *a*, no NADP+; *b*, 0.3:1; *c*, 0.7:1; and *d*, 1:1. The final NADP+ concentration was 1.4 mM. For this titration study, the MurB protein was exchanged into NMR buffer in 100% D_2O and at pH 7.4. The NMR data were collected at 25.0 °C.

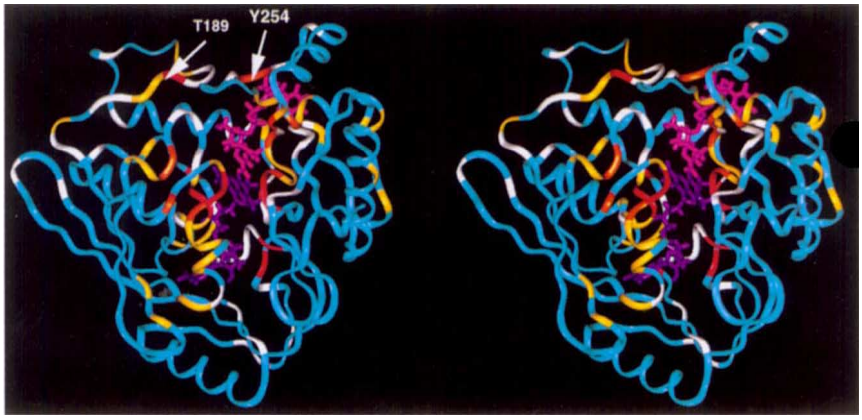

Fig 2 Schematic stereo illustration of the crystal structure of UNAGEP-complexed MurB[3], showing the protein backbone trace and all atoms of UNAGEP (magenta) and FAD (purple). The locations of Thr 189 and Tyr 254 are indicated. White indicates residues (including Pro) to which an HNCO correlation has not been assigned. Blue indicates residues with min (Δ_{ppm}) ≤ 0.1 p.p.m.; yellow, residues with 0.1<min (Δ_{ppm}) ≤0.2 p.p.m.; orange, residues with 0.2 <min (Δ_{ppm}) ≤ 0.3 p.p.m.; and red, residues with min(Δ_{ppm}) >0.3 p.p.m. α_N and α_{CO} normalize the magnitude of ^{15}N and ^{13}CO chemical-shift changes (in p.p.m. units), respectively, to that of $^{1}H_N$ chemical-shift changes. In this study, these scale factors were established from estimates of atom-specific chemical-shift ranges in a protein: 5.5 p.p.m. for $^{1}H_N$; 32 p.p.m. for ^{15}N; and 14 p.p.m. for ^{13}CO. These ranges lead to α_N=0.17 and α_{CO}=0.39.

MurB. However, three potential NADPH/NADP$^+$ binding sites have been proposed based on the crystal structures of substrate-free and UNAGEP-complexed MurB[2,3]. Two of the proposed binding sites[2] would result in a highly unusual hydride transfer to the *si* face[16–18] of the FAD isoalloxazine ring: the first site is coincident with the UNAGEP binding site; the second site involves a smaller channel oriented almost perpendicular to the UNAGEP binding channel. The third binding site[3] proposed for NADPH/NADP$^+$ would result in hydride transfer to the *re* face of the FAD isoalloxazine ring. NADPH binding to this latter site would require a significant movement of a loop containing residue P111.

Ligand binding sites can be localized based on backbone-atom and/or side-chain-atom chemical-shift changes. Chemical-shift-based approaches have traditionally compared actual chemical shifts from both free and ligand-bound forms of the protein to localize the ligand binding site[19–21]. Under this paradigm, localizing the NADP$^+$ binding site on MurB would require complete backbone resonance assignments for NADP$^+$-complexed MurB. Making these assignments is time consuming, especially since NADP$^+$ is in slow exchange with MurB. To circumvent this step, a novel alternative strategy has been pursued that relies only on determining minimum values for backbone-atom chemical-shift changes in MurB incurred upon NADP$^+$ binding.

To measure these minimum chemical-shift changes, 3D HNCO spectra[6] were used instead of ^{1}H-^{15}N HSQC spectra. The HNCO offers increased resonance dispersion while maintaining sufficient sensitivity. Every assigned HNCO correlation from substrate-free MurB is identified with a closest HNCO correlation from NADP$^+$-complexed MurB in terms of a 'p.p.m. distance'. This minimum p.p.m. distance, min(Δ_{ppm}) in equation (1), describes the minimum cumulative chemical-shift change experienced by a given HNCO correlation in response to NADP$^+$ binding:

$$\min(\Delta_{ppm})=\min\{[(^{HN}\Delta_{ppm})^2+(^{N}\Delta_{ppm}*\alpha_N)^2+(^{CO}\Delta_{ppm}*\alpha_{CO})^2]^{1/2}\} \quad (1).$$

$^{HN}\Delta_{ppm}$, $^{N}\Delta_{ppm}$, and $^{CO}\Delta_{ppm}$ are the $^{1}H_N$, ^{15}N and ^{13}CO chemical-shift differences, respectively, between HNCO correlations for substrate-free and NADP$^+$-complexed MurB; the scaling factors α_N and α_{CO} are described in the legend to Fig. 2. Because the minimum chemical-shift approach is qualitative in nature, an exact value for these scale factors is not required. With min(Δ_{ppm}), residues for which the HNCO correlation undergoes a large chemical-shift change are both conservatively and unambiguously identified. For some residues, however, nearby or overlapping peaks may obscure chemical-shift changes due to ligand binding.

Fig. 2 displays min(Δ_{ppm}) values contrast-mapped onto the backbone trace of UNAGEP-complexed MurB[3]. The UNAGEP substrate and FAD cofactor (flavin adenine dinucleotide) are also shown. An interpretation of the chemical-shift changes in MurB upon NADP$^+$ binding must consider the presence of the FAD cofactor. Even if FAD changes only slightly in its relative orientation to the MurB protein in response to NADP$^+$ binding, this slight change can still produce significant differences in local ring currents. With this in mind, Fig. 2 clearly shows that NADP$^+$ binding to MurB induces chemical-shift changes in both UNAGEP and FAD binding pockets. Ala 227 and Gly 228 experience the largest changes, with min(Δ_{ppm}) values of 0.86 and 0.75 p.p.m. respectively. Both residues lie at the bottom of the UNAGEP binding pocket; they are therefore in close proximity to the isoalloxazine ring of FAD. Gln 120, Asn 121, Arg 159 and Asp 160 also show large chemical-shift changes; these residues reside at the FAD/UNAGEP interface region. Smaller changes have been observed for Ser 229–Val 236, Asn 253, Tyr 254 and Val 261–Leu 263; these residues line the UNAGEP binding pocket.

In summary, our evidence suggests the following description of the MurB-NADP$^+$ interaction: (i) structural characteristics of the MurB/FAD interaction in solution change to some degree in response to NADP$^+$ binding; (ii) NADP$^+$ binds to MurB in the same pocket as does UNAGEP; and (iii) NADPH transfers a hydride to the *si* face of the FAD isoalloxazine ring. In addition, Thr 189 shows a substantial chemical-shift change (Fig. 2), with a min(Δ_{ppm}) of 0.33 p.p.m. This residue resides in a loop, which both forms the upper lip of the UNAGEP binding pocket and undergoes a conformational rearrangement upon UNAGEP binding[2]. The substantial chemical-shift change in Thr 189

supports our proposed binding site for NADP+. Recent kinetic experiments also suggest the absence of simultaneous binding to MurB for NADPH and UNAGEP[22]. Finally, the minimum chemical-shift changes reported herein do not support the alternate NADP+ binding sites[2,3]. In context with NADP+ being in slow exchange with MurB, the substantial chemical-shift change in Thr 189 also suggests that both NADP+ binding and UNAGEP binding induce similar structural changes in MurB.

Significance for drug discovery

Structural information on inhibitor binding must be generated rapidly by X-ray crystallography and NMR to benefit structure-assisted drug design. In crystallography, Fourier difference and molecular replacement techniques are well suited to this task. In NMR, an analogous technique, albeit of much lower resolution, is the herein proposed and demonstrated method of minimum chemical-shift changes for localizing ligand binding sites. However, this method still requires backbone resonance assignments for the uncomplexed protein, a process taking up to six months for substrate-free MurB.

If ligand-induced, minimum chemical-shift changes can be mapped and interpreted in perdeuterated large proteins, NMR can contribute both practical and timely structural information towards drug-discovery efforts aimed at larger systems. In this regard, NADP+ is a good ligand because its aromatic moieties generate ring currents that can alter protein chemical shifts. Mapping chemical-shift changes becomes increasingly important in localizing ligand binding sites for the following reason: the number and density of protons may be quite low on many small-molecule drug candidates. Although intermolecular NOEs in protein–ligand complexes provide more definitive and higher resolution structural information, such NOEs may be difficult to observe with both sparsely protonated ligands and perdeuterated proteins. Because four Tyr aromatic rings line the UNAGEP binding site in MurB[3] and because NADP+ has now been shown to bind in the same site as UNAGEP, Tyr residues have been type-specifically protonated[23,24] in an otherwise perdeuterated MurB. With this approach, several intermolecular NOEs have only recently been observed between NADP+ and the MurB protein (data not shown).

Methods

Protein expression and isotopic labelling. MurB (EC 1.1.1.158) from *E. coli* was expressed as a fusion construct with maltose binding protein[14] in minimal medium containing ^{15}N-NH_4SO_4, [$^{13}C_2$]-acetate and 95% D_2O. Additional vitamin supplements were added as described[25]. To insure a complete re-exchange of amide protons following expression in D_2O, the purified MurB protein was subjected to 0.5 M urea in H_2O for 30 min at room temperature at pH 8.0. Following this mild urea treatment, the substrate-free protein was dialysed extensively against the NMR buffer (20 mM d_{15}-Tris-maleate, 0.5 M d_5-glycine, pH 7.2) and then concentrated to 0.6-1.3 mM. The residue numbering for MurB in this report matches that used to describe both published MurB crystal structures. Compared to the crystallized MurB proteins[2,3], however, our MurB protein contains four additional N-terminal residues (IleSerGluPhe), one additional C-terminal residue (Ile) and the following three point substitutions: Y35H, K242E and I279M.

NADP+ binding/titration. For the 3D HNCO spectrum, MurB was complexed with NADP+ in the following manner. A 24 mM stock solution of NADP+ was first prepared in NMR buffer. 25 µl of this stock solution was pipetted into an Eppendorf microfuge tube, to which 340 µl of a 1.39 mM MurB solution was then added. After numerous inversions to establish complete mixing, this solution was transferred by Pasteur pipette back into a Shigemi 5 mm restricted-volume NMR tube. The final NADP+:MurB molar ratio was 1.25:1; the final MurB concentration was 1.3 mM. Similarly, for the ^1H-^{15}N HSQC spectra in Fig. 1, NADP+ was added stepwise to a second MurB sample to achieve the desired NADP+:MurB molar ratios in the titration.

NMR spectroscopy. All NMR data were acquired at 30 °C on Varian UnityPlus 600 MHz NMR spectrometers unless otherwise stated. Data were processed using either VNMR 5.1 (Varian Associates, Palo Alto, CA) or an extensively modified version[26] of FELIX 1.0 (Hare Research, Inc., Bothell, WA).

Bennett T. Farmer II[1], Keith L. Constantine[1], Valentina Goldfarb, Mark S. Friedrichs, Michael Wittekind, Joseph Yanchunas, Jr., James G. Robertson and Luciano Mueller
Pharmaceutical Research Institute, Bristol-Myers Squibb Co. P.O. Box 4000
Princeton, New Jersey 08543-4000, USA
[1]These two authors contributed equally.

Correspondence should be addressed to B.T.F.
sandy@atlas.bms.com

Received 24 June; accepted 30 August 1996.

Acknowledgements
The authors gratefully acknowledge P.J. Falk, H.-T. Ho, M. Pucci and T. Dougherty for the MurB clone, expression system and initial purification scheme.

1. Benson, T.E., Marquardt, J.L., Marquardt, A.C., Etzkorn, F.A. & Walsh, C.T. *Biochemistry* **32**, 2024–2030 (1993).
2. Benson, T.E., Walsh, C.T. & Hogle, J.H. *Structure* **4**, 47–54 (1996).
3. Benson, T.E., Filman, D.J., Walsh, C.T. & Hogle, J.M. *Nature Struct. Biol.* **2**, 644–653 (1995).
4. Muchmore, D.C., McIntosh, L.P., Russell, C.B., Anderson, D.E. & Dahlquist, F.W. *Meths. Enzymol.* **177**, 44–73 (1989).
5. Venters, R.A., Calderone, T.L., Spicer, L.D. & Fierke, C.A. *Biochemistry* **30**, 4491–4494 (1991).
6. Kay, L.E., Ikura, M., Tschudin, R. & Bax, A. *J. Magn. Reson.* **89**, 496–514 (1990).
7. Montelione, G.T., Lyons, B.A., Emerson, S.D. & Tashiro, M. *J. Am. Chem. Soc.* **114**, 10974–10975 (1992).
8. Kay, L.E., Clore, G.M., Bax, A. & Gronenborn, A.M. *Science* **249**, 411–414 (1990).
9. Zuiderweg, E.R.P., Petros, A.M., Fesik, S.W. & Olejniczak, E.T. *J. Am. Chem. Soc.* **113**, 370–372 (1991).
10. Grzesiek, S., Anglister, J., Ren, H. & Bax, A. *J. Am. Chem. Soc.* **115**, 4369–4370 (1993).
11. Yamazaki, T., Lee, W., Arrowsmith, C.H., Muhandiram, D.R. & Kay, L.E. *J. Am. Chem. Soc.* **116**, 11655–11666 (1994).
12. Venters, R.A., Metzler, W.J., Spicer, L.D., Mueller, L. & Farmer II, B.T. *J. Am. Chem. Soc.* **117**, 9592–9593 (1995).
13. Yamazaki, T. *et al. J. Am. Chem. Soc.* **116**, 6464–6465 (1994).
14. Pucci, M.J., Discotto, L.F. & Dougherty, T.J. *J. Bacteriol.* **174**, 1690–1693 (1992).
15. Constantine, K.L. *et al. Proteins Struct. Funct. Genet.* **15**, 290–311 (1993).
16. Manstein, D.J., Pai, E.F., Schopfer, L.M. & Massey, V. *Biochemistry* **25**, 6807–6816 (1986).
17. Ghisla, S. & Massey, V. *Eur. J. Biochem.* **181**, 1–17 (1989).
18. Sumner, J.S. & Matthews, R.G. *J. Am. Chem. Soc.* **114**, 6949–6956 (1992).
19. Neri, P. *et al. FEBS Letters* **294**, 81–88 (1991).
20. Görlach, M., Wittekind, M., Beckman, R.A., Mueller, L. & Dreyfuss, G. *EMBO J.* **11**, 3289–3295 (1992).
21. Newkirk, K. *et al. Proc. Natl. Acad. Sci. USA* **91**, 5114–5118 (1994).
22. Dhalla, A.M. *et al. Biochemistry* **34**, 5390–5402 (1995).
23. Oda, Y., Nakamura, H., Yamazaki, T. & Nagayama, K. *J. Biomol. NMR* **2**, 137–147 (1992).
24. Metzler, W.J., Wittekind, M., Goldfarb, V., Mueller, L. & Farmer II, B.T. *J. Am. Chem. Soc.* **118**, 6800–6801 (1996).
25. Venters, R.A. *et al. J. Biomol. NMR* **5**, 339–344 (1995).
26. Friedrichs, M.S., Mueller, L. & Wittekind, M. *J. Biomol. NMR* **4**, 703–726 (1994).